



Fabrication and whispering gallery resonance of self-rolled up gallium nitride microcavities



Jiao Wang^{a,b}, Enming Song^b, Chunlei Yang^c, Lirong Zheng^{a,d}, Yongfeng Mei^{b,*}

^a School of Information Science & Engineering, Fudan University, Shanghai 200433, PR China

^b Department of Materials Science, Fudan University, Shanghai 200433, PR China

^c Center for Photovoltaic Solar Cells, Shen Zhen Institute of Advanced Technology, Chinese Academy of Sciences, Shenzhen 518055, PR China

^d School of Information and Communication Technologies, Royal Institute of Technology, 164 40 Stockholm, Sweden

ARTICLE INFO

Article history:

Received 20 October 2016

Received in revised form 11 February 2017

Accepted 25 February 2017

Available online 1 March 2017

Keywords:

GaN

Microtube

Rolled-up

Whispering gallery mode (WGM)

ABSTRACT

The C-plane monocrystalline GaN/ZnO thin film epitaxially grows on A-plane sapphire substrate by molecular beam epitaxy (MBE) is revealed by the reflection high-energy electron diffraction (RHEED). The monocrystalline GaN nanomembranes have been rolled up into tubular microstructures as whispering gallery microcavities, which support the whisper gallery modes (WGMs) in the violet and blue regime. The WGMs of the rolled-up monocrystalline GaN devices are tunable with microtube diameter by tuning the strain gradient of the GaN nanomembranes. This approach could help with not only the further development of GaN-based photonic devices, but also the physical understanding of other rolled-up optical microcavities.

© 2017 Elsevier B.V. All rights reserved.

1. Introduction

Gallium nitride (GaN), as one direct bandgap semiconductor with excellent optical properties, acts as the leading material for the application for optoelectronic devices [1], particularly ultraviolet (UV) and visible micro-/nanoscale light sources operating at room temperature [2–6]. However, the progress of GaN-based optical microdevices is still demanding the fabrication of high quality freestanding GaN layers and enabling them to be shaped and assembled into new structures and devices [6–9]. Recently, UV-assisted electroless chemical etching [1], chemical lift-off [10], in-situ lift-off [11,12], or laser lift-off [13] have been also proposed to achieve high quality free-standing GaN layers or membranes. However, the residual strains during growth and process could lead to dislocations and macroscopic cracks [11,14,15]. Hence, effective strain-engineering can help the preparation of high-quality GaN-based nanobelts [16] or high quality free-standing GaN wafer (350 μm) [17]. Recently, strain-engineering is also adopted for shaping single/composite nanomembranes into size-scalable three-dimensional (3D) architectures due to the elastic energy minimization [18,19]. Rolled-up micro- and nanoscale tubular optical cavities can be realized by standard photolithography and etching process based on the design of sacrificial layers [18]. The luminescent spectra and the light confinement in such ring-like optical resonators are tunable by modifying the functional layer materials, designing the complex 3D

geometry and surface modification [8,18]. Various interesting materials were used for the fabrication of self-rolled up tubular optical microcavities at difference spectral range. As for oxide self-rolled up optical microcavities, their luminescent spectra in yellow and red region are attributed to defect center, such as SiO_x/Si [20], SiO_x/SiO₂ [21], Y₂O₃/ZrO₂ [22], and TiO₂ [22], etc. (Fig. 1). The high index semiconductor self-rolled up microcavities based on InGaAs quantum wells (InGaAs QW) [23–25] and PbS quantum dots (PbS QD) [26] show typical whisper gallery modes (WGMs) with high quality-factor (Q-factor) and 3D light confinement in near infrared region (Fig. 1). Recently, the WGMs with high Q-factor of luminescent Cd₆P₇ nanoparticles embedded TiO₂ microtube cavities extend from the visible to the near infrared [27]. Although previous theoretical and experimental results on GaN-based rolled-up micro-/nano-tubes have largely focused on the design of the tube structure [7,8,28], there is no report on rolled-up tubular optical microcavities based on GaN material for the resonance in the range of violet and blue.

In this work, we develop an effective process for fabricating GaN-based tubular optical microcavities by the rolling of single crystal GaN nanomembranes. The typical photoluminescence spectra of self-rolled up GaN microtube at room temperature indicated that these GaN microtubes support the WGMs in the violet and blue regime. We fabricate tubular GaN optical microcavities with WGMs through the self-rolled up nanotechnology by releasing of thin c-oriented GaN epilayer from A-plane sapphire substrate with a sacrificial ZnO layer. Our approach hints an interesting method to build up GaN-based photonic devices.

* Corresponding author.
E-mail address: yfm@fudan.edu.cn (Y. Mei).

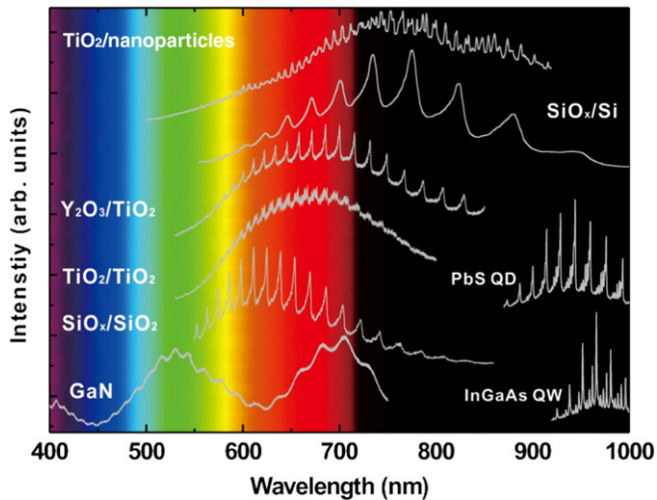


Fig. 1. The micro-photoluminescence (μ -PL) spectra of rolled-up microtubes in various color regions, which are composed of SiO_x/Si ($Q < 100$) [20], $\text{SiO}_x/\text{SiO}_2$ ($Q \sim 100$) [21], $\text{Y}_2\text{O}_3/\text{ZrO}_2$ ($Q > 1500$) [22], TiO_2 ($Q > 1500$) [22], InGaAs QW ($Q > 2000$) [23,24], PbS QD ($Q > 1000$) [26], $\text{TiO}_2/\text{nanoparticles}$ ($Q > 1200$) [27] and GaN (this work, $Q \sim 100$).

2. Experimental procedure

2.1. Synthetic procedures

Self-rolled-up tubular GaN optical microcavities with WGMs are fabricated by releasing of thin GaN epilayer from A -plane sapphire substrate with a ZnO sacrificial layer. ZnO layer (i.e. sacrificial layer) and GaN film were grown by plasma-assisted molecular beam epitaxy (MBE). A ZnO buffer layer is grown directly on A -plane sapphire substrates at 380°C . The oxygen (O_2) flow rate and plasma power are kept constant at 4 sccm and 380 W, respectively. Then, the high quality ZnO epilayer (~ 180 nm) are grown at 700°C with growth rate of 2.8 nm min^{-1} . The oxygen (O_2) flow rate and plasma power are kept constant at 6 sccm and 400 W, respectively. A GaN layer is then grown on top of the high quality ZnO layer at 780°C with nitrogen (N_2) flow rate at 3 sccm and plasma power at 350 W. In order to construct self-

rolled-up GaN optical microcavities, the ZnO layer were employed as a sacrificial layer. In fact, the ZnO layer can be easily etched by HCl (1.7 mol L^{-1}) or KOH (4 mol L^{-1}) solutions.

2.2. Sample characterization

The crystal structural quality of the samples is studied in situ by reflection high-energy electron diffraction (RHEED), and by high resolution X-ray diffraction (HRXRD) and transmission electron microscope (TEM) techniques after the growth. The morphologies of GaN microtubes are detected by scanning electron microscopy (SEM) and optical microscope. The optical properties of the fabricated microtubes were tested by the micro-photoluminescence (μ -PL) setup at room temperature.

3. Results and discussion

The sample composed of the layer sequence of sapphire substrate, ZnO and GaN from bottom to top. The fabrication process of tubular self-rolled up micro-cavities is schematically displayed in Fig. 2a. We design our experiments as following: the c -oriented ZnO layer can be selectively removed, releasing the active GaN layer, since the intrinsic stress gradient existing in the GaN active nanomembrane can cause it to self-assemble into a micro-tubular cavity as shown in Fig. 2a. Our sample started with the ideal A -plane of sapphire substrate, which is twofold symmetric, while the C -plane of ZnO and GaN is six-fold symmetric. However, in such systems, single crystalline thin films can be epitaxially grown by the so-called domain matching epitaxy (DME), where integral multiples of major lattice planes match across the film-substrate interface [15,29]. For GaN and ZnO layers, the 4-fold of the GaN or ZnO a lattice constant fits perfectly to the c lattice constant of sapphire, three GaN or ZnO ($1\bar{1}00$) planes fit to two sapphire ($1\bar{1}00$) planes in other direction [15,30,31]. Thus, c -oriented ZnO layer and GaN layer can be grown on the A -plane sapphire substrate.

The surface reconstructions of ZnO and GaN observed by reflection high-energy electron diffraction (RHEED) are adopted to monitor the ZnO buffer layer and GaN thin film surface during growth. Fig. 2b and c show RHEED patterns observed at the surface of the GaN/ZnO film

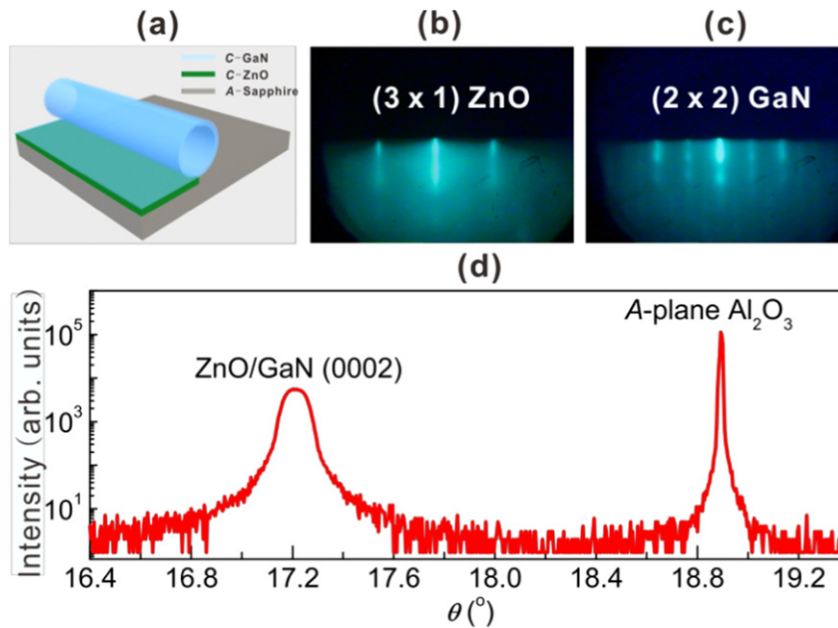


Fig. 2. (a) Schematic diagram illustrating the fabrication process of a rolled-up C -plane GaN tubular microcavity on A -plane sapphire substrate. RHEED pattern show the surface reconstruction of (b) ZnO and (c) GaN . (d) high resolution X-ray diffraction (HRXRD) spectra of the as-grown GaN film on ZnO/A -plane sapphire substrate. All the diffraction angle are calibrated by the A -plane sapphire substrate ($11\bar{2}0$).

during growth. The RHEED pattern of a firstly-grown ZnO layer clearly indicated that the surface (3×1) reconstruction (Fig. 2b) correspond to a clean, high quality O-ZnO (0001) surface [32]. After the GaN film growth, it is found that the transition for the appearance of the reconstruction pattern as presented in Fig. 2c. This reconstruction can be explained by a (2×2) reconstruction unit mesh of the GaN film on the (0001) surface (Fig. 2c), a structure with surface features of spacing twice than that of the unit cell. This (2×2) reconstruction has been previously observed and corresponds to a stable growth front for achieving good quality epitaxial GaN layers by plasma-assisted molecular beam epitaxy (MBE) [33]. Fig. 2d shows the rocking curve of the (0002) plane for the ZnO/GaN thin film grown on the A-plane sapphire substrate. The {0001} plane of the GaN film grown on an A-plane sapphire substrate is parallel to the $\{11\bar{2}0\}$ face of the A-plane sapphire. One side of the hexagonal GaN crystal is parallel to the C-plane of the A-plane sapphire substrate [34].

Lift-off process was performed by immersing a GaN/ZnO/A- Al_2O_3 sample in dilute HCl (1.7 mol L^{-1}) or KOH (4 mol L^{-1}) solutions after a mechanical delimitation of submillimetric mesas with a diamond scribe (see the Experimental procedure Section). Fig. 3a shows typical optical microscope images of rolled-up GaN microtubular structures.

During the chemical lift-off process, the ZnO dissolved completely and the freestanding GaN nanomembrane released and spontaneously formed into microtubes on the A-plane sapphire substrate (Fig. 3b). However, the GaN layers grown on the C-plane sapphire could not roll into microtubes. This result indicated that the sapphire surface orientation has great influence on the GaN nanomembranes reconstruction.

For the epitaxial growth of GaN/ZnO layer on $(11\bar{2}0)$ (A-plane) sapphire substrate, the lattice mismatch is much smaller than in the case of epitaxy on (0001), the difference in the planar symmetry in this case results in anisotropy high-strained GaN/ZnO layer [14]. The rolling of GaN nanomembranes is ascribed to the residual strain gradient in GaN layer [19]. The in-plane strain of GaN/ZnO epilayers grown on A-plane sapphire is expected to be anisotropic due to the different thermal expansion coefficients of sapphire in the directions parallel and perpendicular to its *c*-axis, as well as due to the nonequal lattice mismatches along these two directions [15]. For the DME, due to the in-plane anisotropic biaxial strain and the small thickness of ZnO layer ($\sim 180 \text{ nm}$), we expect that the hexagonal basal plane of GaN with $\sim 55 \text{ nm}$ (Fig. 3d) in thickness grown on ZnO layer is also distorted [15]. For the DME condition, the epitaxy is not straightforward, since the epitaxial plane of C-plane GaN does not share the same symmetry as that of A-plane

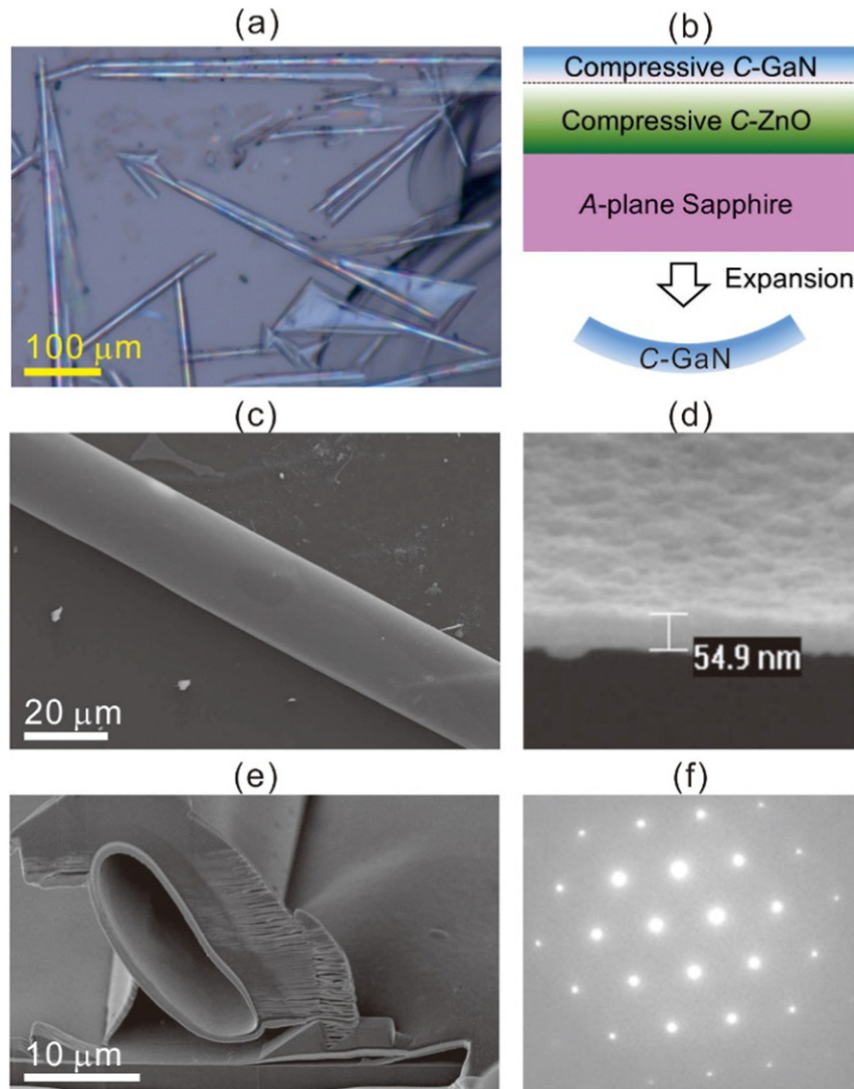


Fig. 3. (a) Optical microscope images of rolled-up GaN microtubes. (b) Schematic representation of rolling up for C-plane GaN nanomembranes on A-plane sapphire substrate. The GaN and ZnO layer with a compressive strain gradient grown on A-plane sapphire substrate. SEM images for (c) a GaN microtube, (d) cross-section of a GaN thin film with the thickness of $\sim 55 \text{ nm}$ and (e) cross-section of a GaN microtube. (f) Selective area diffraction pattern of the wall of GaN microtube.

sapphire [14,29]. The difference in the planar symmetry in this case results in anisotropy high-strained GaN/ZnO layer [14,19]. Meanwhile, due to the nonequal lattice mismatches along these two directions during DME process, the defects in GaN epilayer on *A*-plane sapphire substrate are inevitable [14]. Most of the defects are confined near the GaN/ZnO interface. Hence, the residual dislocation decreases along the growth direction is consistent with the generation of the strain gradient in our GaN layer. In our experimental condition, the thermal stress, lattice mismatch and interdiffusion between GaN and ZnO are three possible origins cause compressive stress in GaN layer. Thus, in this GaN/ZnO/*A*-Al₂O₃ system, the total final residual strain gradient in GaN layer is anisotropy compressive [19,35]. The anisotropic compressive strain gradient is responsible for the GaN nanomembranes rolling up [15,19]. Fig. 3b indicates a schematic to illustrate the rolling up of *C*-plane GaN nanomembranes on *A*-plane sapphire substrate. The strain magnitude gradually decreases from GaN epilayer/ZnO sacrificial layer interface to the GaN epilayer surface. The releasing GaN epilayer with the compressive strain gradient from the *A*-plane sapphire causes a net bending force to bend the GaN epilayer upward [19]. This self-rolled up mechanism of GaN microtubes is consistent with the roll-up mechanism in previous report [19]. Fig. 3c–e shows the scanning electron microscopy (SEM) images of GaN microtube. The thickness of GaN nanomembranes is about 55 nm (Fig. 3d). And the cross-section image of the microtube with several rolling was shown in Fig. 3e (the deformation of microtube caused by the focused ion beam milling). The selective area diffraction pattern of the wall of GaN microtube image from the obtained diffraction image of flat areas of the tube (not shown), a highly textured growth in the $\langle 0001 \rangle$ direction is expected and observed as revealed in Fig. 3f. The quality of GaN film with different luminescent properties can be improved with the defects reduced by optimized the epitaxial parameters, such as gas flow rate, plasma power, and substrate temperature.

After demonstrating the crystalline nature and the 3D architecture of the self-rolled up GaN microtubes, we further characterize their luminescence property using μ -PL spectra. All the ZnO sacrificial layers were removed during the chemical etching step, then the GaN microtubes were formed on the *A*-plane sapphire substrate. Thus, the influence from the ZnO layer on the μ -PL signal was removed. Fig. 4 shows the typical μ -PL spectra from the tubular GaN microtubes with different diameters. The WGM peaks are observed from the rolled-up GaN microtubes as optical microcavities with different tube diameters (6–15 μ m). These μ -PL spectra indicate a good coupling between the

typical GaN PL emission and the optical resonance modes in visible region (3.1–1.653 eV, 400–750 nm, Figs. 1 and 4) covering violet and blue. There are three main emission bands in the μ -PL spectra. The μ -PL peak emission at approximately 3.1 eV (~400 nm, violet) is the characteristic band to band transition in GaN. Meanwhile, the μ -PL peak emissions from these GaN microtubes demonstrates two broad emission at approximately 1.8 eV (red luminescence, RL2, ~690 nm) and 2.35 eV (green luminescence, GL2, ~530 nm), respectively. These RL2 and GL2 bands were observed in GaN by other groups [36,37]. The defects responsible for the RL2 and GL2 bands are native defects or complexes related to excess Ga, presumably deep compensating acceptors [36]. The Ga_N defect (excess Ga in N positions) is one probable candidate since it is predicted to be a double acceptor with a large outward relaxation around it and with the energy level close to the middle of the band gap [36]. It is also possible that the RL2 and/or GL2 bands result from the transitions from the excited state of the defects to the ground state [30]. Mode-like peaks can be observed and superimposed onto such broad luminescence band of the GaN layer. Each peak corresponds to a WGM with an azimuthal number *m*. As shown in Fig. 4, the GaN microtubes with different diameters show different WGMs resonance spectra. For functional device application of tubular microcavities, the Q-factor is very important. As one of most basic parameters, the Q-factor is a measure of the energy loss and defined by the time-averaged energy in the cavity divided by the energy loss per cycle [38, 39]. The Q-factors of these GaN microtubes are quite low (~100), which is mainly attributed to the surface roughness, tiny wall thickness, and structure defects (Fig. 3). The Q-factor could be improved by optimized growth parameters (e.g. film thickness and surface roughness) and roll-up process (looseness of structure) [38,40].

Normally, the resonance position (*v*, eV) exhibits a linear dependency on mode numbers (*m*). The free spectral range (FSR) is inversely proportional with microtube diameter (*D*) according to $\Delta v_{FSR} = c / (\pi n_{eff} D)$ or $\Delta \lambda_{FSR} = \lambda^2 / (\pi n_{eff} D)$, where *c* is the speed of light, λ is the resonance position (nm), and *n_{eff}* is the effective refractive index. Thus, for a certain microtube with given diameter, the experimental Δv_{FSR} (eV) keeps constant with the changing of mode number and resonance position (*v*, eV). The FSRs of the rolled up GaN microtubes with different diameter are shown in Fig. 5. It is found that the measured FSRs of tubular microcavities with various diameters decrease with the increasing of diameters. Then, mode number *m* can be calculated according to $m = v / \Delta v_{FSR} = (\pi n_{eff} D) / \lambda$, where *v* is the resonance position (eV). The effective refractive index *n_{eff}* of the wall of these GaN microtubes (lower than 1.2) is calculated according to $m = (\pi n_{eff} D) / \lambda$. These *n_{eff}* are quite lower than the refractive index of bulk GaN (*n* = 2.429), due to the surface roughness, tiny thickness of the wall of GaN microtube, and structure defects (Fig. 3).

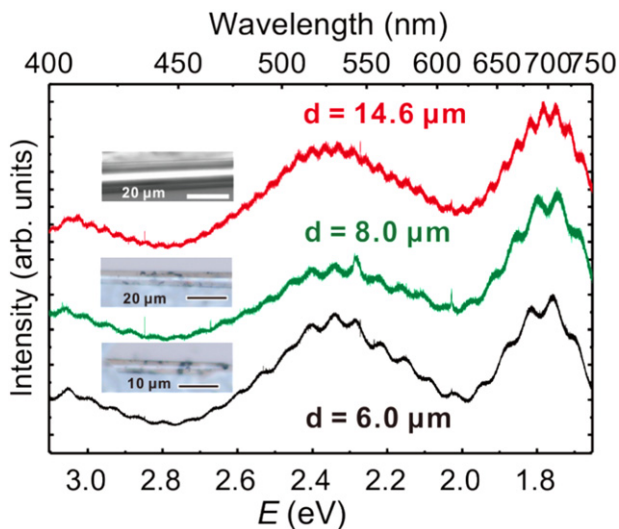


Fig. 4. Measured μ -PL spectra of the rolled up GaN microtubes with different diameter. Optical microscope images of rolled-up GaN microtubes with different diameter are shown as insets.

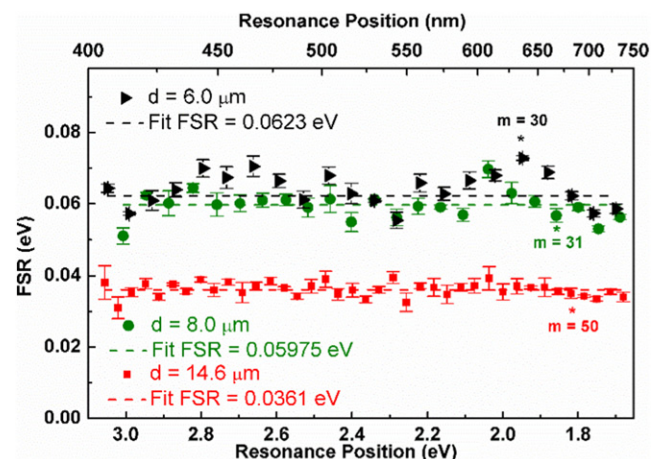


Fig. 5. FSR of rolled up GaN microtubes with different diameters.

4. Conclusions

In conclusion, we demonstrate a chemical lift-off process of the GaN nanomembranes released from the A-plane Al₂O₃ substrate with a ZnO sacrificial layer via the immersion into a dilute HCl or KOH solution. Freestanding GaN nanomembranes self-rolled up into microtubes and performed as optical microcavities. Such an approach represents a straight forward, wet etching method to obtain GaN optical microcavity with the resonance in the range of violet and blue. Our method might promise a practical route for the realization of tubular GaN microcavity, which can be applied to construct other GaN-based photonic devices.

Acknowledgements

This work is supported by the Natural Science Foundation of China [Nos. 51322201, U1632115 and 51302039], and Science and Technology Commission of Shanghai Municipality [No. 12520706300].

References

- [1] R.T. ElAfandy, M.A. Majid, T.K. Ng, L. Zhao, D. Cha, B.S. Ooi, Exfoliation of threading dislocation-free, single-crystalline, ultrathin gallium nitride nanomembranes, *Adv. Funct. Mater.* 24 (2014) 2305–2311.
- [2] C.T. Lee, C.J. Cheng, H.Y. Lee, Y.C. Chu, Y.H. Fang, C.H. Chao, M.H. Wu, Color conversion of GaN-based micro light-emitting diodes using quantum dots, *IEEE Photon. Technol. Lett.* 27 (2015) 2296–2299.
- [3] G. Sarau, M. Heilmann, M. Latzel, S. Christiansen, Disentangling the effects of nanoscale structural variations on the light emission wavelength of single nano-emitters: InGa_N/GaN multi-quantum well nano-LEDs for a case study, *Nanoscale* 6 (2014) 11953–11962.
- [4] H. Nakazato, H. Kawaguchi, A. Iwabuchi, K. Hane, Micro fluorescent analysis system integrating GaN-light-emitting-diode on a silicon platform, *Lab Chip* 12 (2012) 3419–3425.
- [5] T.I. Kim, Y.H. Jung, J. Song, D. Kim, Y. Li, H.S. Kim, I.S. Song, J.J. Wierer, H.A. Pao, Y. Huang, J.A. Rogers, High-efficiency, microscale GaN light-emitting diodes and their thermal properties on unusual substrates, *Small* 8 (2012) 1643–1649.
- [6] T. Wang, K.B. Lee, J. Bai, P.J. Parbrook, F. Ranalli, Q. Wang, R.J. Airey, A.G. Cullis, H.X. Zhang, D. Massoubre, Z. Gong, I.M. Watson, E. Gu, M.D. Dawson, The 310–340 nm ultraviolet light emitting diodes grown using a thin GaN interlayer on a high temperature AlN buffer, *J. Phys. D: Appl. Phys.* 41 (2008) 094003.
- [7] Y. Takagaki, Y.J. Sun, O. Brandt, K.H. Ploog, Strain relaxation in AlN/GaN bilayer films grown on g-LiAlO₂(100) for nanoelectromechanical systems, *Appl. Phys. Lett.* 84 (2004) 4756–4758.
- [8] Y. Mei, D.J. Thurmer, C. Deneke, S. Kiravittaya, Y.F. Chen, A. Dadgar, F. Bertram, B. Bastek, A. Krost, J. Christen, T. Reindl, M. Stoffel, E. Coric, O.G. Schmidt, Fabrication, self-assembly, and properties of ultrathin AlN/GaN porous crystalline nanomembranes: tubes, spirals, and curved sheets, *ACS Nano* 3 (2009) 1663–1668.
- [9] K.J. Lee, M.A. Meitl, J.-H. Ahn, J.A. Rogers, R.G. Nuzzo, V. Kumar, I. Adesida, Bendable GaN high electron mobility transistors on plastic substrates, *J. Appl. Phys.* 100 (2006) 124507.
- [10] D.J. Rogers, F.H. Teherani, A. Ougazzaden, S. Gautier, L. Divay, A. Lusso, O. Durand, F. Wyczisk, G. Garry, T. Monteiro, M.R. Correia, M. Peres, A. Neves, D. McGrouther, J.N. Chapman, M. Razeghi, Use of ZnO thin films as sacrificial templates for metal organic vapor phase epitaxy and chemical lift-off of GaN, *Appl. Phys. Lett.* 91 (2007) 071120.
- [11] S.W. Lee, T. Minegishi, W.H. Lee, H. Goto, H.J. Lee, S.H. Lee, H.J. Lee, J.S. Ha, T. Goto, T. Hanada, M.W. Cho, T. Yao, Strain-free GaN thick films grown on single crystalline ZnO buffer layer with in situ lift-off technique, *Appl. Phys. Lett.* 90 (2007) 061907.
- [12] F. Lipski, S.B. Thapa, J. Hertkorn, T. Wunderer, S. Schwaiger, F. Scholz, M. Feneberg, M. Wiedenmann, K. Thonke, H. Hochmuth, M. Lorenz, M. Grundmann, Studies towards freestanding GaN in hydride vapor phase epitaxy by in-situ etching of a sacrificial ZnO buffer layer, *Phys. Status Solidi C* 6 (2009) S352.
- [13] G. Martinez-Criado, M. Kuball, M. Benyoucef, A. Sarua, E. Frayssinet, B. Beaumont, P. Gibart, C.R. Miskys, M. Stutzmann, Free-standing GaN grown on epitaxial lateral overgrown GaN substrates, *J. Cryst. Growth* 255 (2003) 277–281.
- [14] D. Doppalapudi, E. Iliopoulos, S.N. Basu, T.D. Moustakas, Epitaxial growth of gallium nitride thin films on A-plane sapphire by molecular beam epitaxy, *J. Appl. Phys.* 85 (1999) 3582–3589.
- [15] H. Kim-Chauveau, P. De Mierry, H. Cabane, D. Gindhart, In-plane anisotropy characteristics of GaN epilayers grown on A-face sapphire substrates, *J. Appl. Phys.* 104 (2008) 113516.
- [16] H.F. Liu, W. Liu, S.J. Chua, D.Z. Chi, Fabricating high-quality GaN-based nanobelts by strain-controlled cracking of thin solid films for application in piezotronics, *Nano Energy* 1 (2012) 316–321.
- [17] N. Lin, J. Wu, H. Xu, N. Liu, T. Zheng, W. Lin, C. Liu, D. Cai, In situ self-release of thick GaN wafer from sapphire substrate via graded strain field engineering, *Appl. Phys. Lett.* 104 (2014) 012110.
- [18] G. Huang, Y. Mei, Thinning and shaping solid films into functional and integrative nanomembranes, *Adv. Mater.* 24 (2012) 2517–2546.
- [19] R. Songmuang, C. Deneke, O.G. Schmidt, Rolled-up micro- and nanotubes from single-material thin films, *Appl. Phys. Lett.* 89 (2006) 223109.
- [20] R. Songmuang, A. Rastelli, S. Mendach, O.G. Schmidt, SiO₂/Si radial superlattices and microtube optical ring resonators, *Appl. Phys. Lett.* 90 (2007) 091905.
- [21] G.S. Huang, S. Kiravittaya, V.A. Bolaños Quiñones, F. Ding, M. Benyoucef, A. Rastelli, Y.F. Mei, O.G. Schmidt, Fabrication and optical properties of C/β-SiC/Si hybrid rolled-up microtubes, *Appl. Phys. Lett.* 94 (2009) 141901.
- [22] J. Wang, T. Zhan, G. Huang, X. Cui, X. Hu, Y. Mei, Tubular oxide microcavity with high-index-contrast walls: Mie scattering theory and 3D confinement of resonant modes, *Opt. Express* 20 (2012) 18555–18567.
- [23] C. Strelow, H. Rehberg, C.M. Schultz, H. Welsch, C. Heyn, D. Heitmann, T. Kipp, Optical microcavities formed by semiconductor microtubes using a bottle-like geometry, *Phys. Rev. Lett.* 101 (2008) 127403.
- [24] T. Kipp, H. Welsch, C. Strelow, C. Heyn, D. Heitmann, Optical modes in semiconductor microtube ring resonators, *Phys. Rev. Lett.* 96 (2006) 077403.
- [25] Z. Tian, V. Veerasubramanian, P. Bianucci, S. Mukherjee, Z. Mi, A.G. Kirk, D.V. Plant, Single rolled-up InGaAs/GaAs quantum dot microtubes integrated with silicon-on-insulator waveguides, *Opt. Express* 19 (2011) 12164–12171.
- [26] K. Dietrich, C. Strelow, C. Schliehe, C. Heyn, A. Stemmann, S. Schwaiger, S. Mendach, A. Mews, H. Weller, D. Heitmann, T. Kipp, Optical modes excited by evanescent-wave-coupled PbS nanocrystals in semiconductor microtube bottle resonators, *Nano Lett.* 10 (2010) 627–631.
- [27] A. Madani, L. Ma, S. Miao, M.R. Jorgensen, O.G. Schmidt, Luminescent nanoparticles embedded in TiO₂ microtube cavities for the activation of whispering-gallery-modes extending from the visible to the near infrared, *Nanoscale* 8 (2016) 9498–9503.
- [28] M. Djavid, X. Liu, Z. Mi, Improvement of the light extraction efficiency of GaN-based LEDs using rolled-up nanotube arrays, *Opt. Express* 22 (2014) A1680–A1686.
- [29] J. Narayan, B.C. Larson, Domain epitaxy: a unified paradigm for thin film growth, *J. Appl. Phys.* 93 (2003) 278–285.
- [30] P. Fons, I. Kwata, A. Yamada, K. Matsubara, S. Niki, K. Nakahara, T. Tanabe, H. Takasu, Uniaxial locked epitaxy of ZnO on the a face of sapphire, *Appl. Phys. Lett.* 77 (2000) 1801–1803.
- [31] Y. Xie, M. Madel, T. Zoberbier, A. Reiser, W. Jie, B. Neuschl, J. Biskupek, U. Kaiser, M. Feneberg, K. Thonke, Enforced c-axis growth of ZnO epitaxial chemical vapor deposition films on A-plane sapphire, *Appl. Phys. Lett.* 100 (2012) 182101.
- [32] M. Kunat, S. Gil Giroi, T. Becker, U. Burghaus, C. Woll, Stability of the polar surfaces of ZnO: a reinvestigation using He-atom scattering, *Phys. Rev. B* 66 (2002) 081402.
- [33] P. Hacke, G. Feuillet, H. Okumura, S. Yoshida, Monitoring surface stoichiometry with the (2 × 2) reconstruction during growth of hexagonal-phase GaN by molecular beam epitaxy, *Appl. Phys. Lett.* 69 (1996) 2507–2509.
- [34] A. Alemu, B. Gil, M. Julier, S. Nakamura, Optical properties of wurtzite GaN epilayers grown on A-plane sapphire, *Phys. Rev. B* 57 (1998) 3761–3764.
- [35] T. Minegishi, T. Suzuki, C. Harada, H. Goto, M.W. Cho, T. Yao, Stress dependence on N/Ga ratio in GaN epitaxial films grown on ZnO substrates, *Curr. Appl. Phys.* 4 (2004) 685–687.
- [36] M.A. Reshchikov, H. Morkoc, Luminescence properties of defects in GaN, *J. Appl. Phys.* 97 (2005) 061301.
- [37] D.M. Hofmann, B.K. Meyer, H. Alves, F. Leiter, W. Burkhard, N. Romanov, Y. Kim, J. Kruger, E.R. Weber, The red (1.8 eV) luminescence in epitaxially grown GaN, *Phys. Status Solidi A* 180 (2000) 261–265.
- [38] J. Wang, T.R. Zhan, G.S. Huang, P.K. Chu, Y.F. Mei, Optical microcavities with tubular geometry: properties and applications, *Laser Photonics Rev.* 8 (2014) 521–547.
- [39] F. Zhao, T. Zhan, G. Huang, Y. Mei, X. Hu, Liquid sensing capability of rolled-up tubular optical microcavities: a theoretical study, *Lab Chip* 12 (2012) 3798–3802.
- [40] E.J. Smith, S. Schulze, S. Kiravittaya, Y. Mei, S. Sanchez, O.G. Schmidt, Lab-in-a-tube: detection of individual mouse cells for analysis in flexible Split-Wall microtube resonator sensors, *Nano Lett.* 11 (2011) 4037.